

## COMMUNICATION

# Exceptional activity of sub-nm Pt clusters on CdS for photocatalytic hydrogen production: A combined of experimental and first-principles study †

Cite this: DOI: 10.1039/x0xx00000x

Received 00th January 2012,  
Accepted 00th January 2012Qiyuan Wu,<sup>a</sup> Shangmin Xiong,<sup>a</sup> Peichuan Shen,<sup>a</sup> Shen Zhao,<sup>a</sup> Yan Li,<sup>a, b</sup> Dong Su,<sup>a, c</sup> and Alexander Orlov<sup>a\*</sup>

DOI: 10.1039/x0xx00000x

[www.rsc.org/](http://www.rsc.org/)

**In this work we have explored a new concept of substantially increasing photocatalytic activity for H<sub>2</sub> production of conventional semiconductors by modifying them with sub-nm Pt particles. By combining both experimental and theoretical approaches we have also developed new mechanistic insights into the 17 times increase in photocatalytic activity of Pt modified CdS catalysts.**

Photocatalytic water splitting is a very dynamic field offering a pathway for production of hydrogen in a sustainable way. There are already several exciting developments resulting in new photocatalysts with substantially improved quantum efficiency for H<sub>2</sub> production.<sup>1-6</sup> In addition to modifying the main catalysts, there is also a strategy of using nanoparticles (NPs) as co-catalysts to increase the rate of reaction. Among many known co-catalysts for H<sub>2</sub> evolution, noble metals such as Pt, Rh, and Au are among the most promising ones.<sup>4-8</sup> However, most of the research on the use of noble metal NP co-catalysts has been focused on the particle size of above 1-2 nm, where catalytic properties are primarily derived from the metallic character of these NPs. There is also a bigger question of whether the size of Pt clusters has any significant effect on catalytic activity. On one hand, Jun *et al.* investigated the size effect of Pt NPs on photocatalytic activity of TiO<sub>2</sub>, and no significant correlation between size (within 1.47 nm to 2.88 nm range) and catalytic activity of Pt NPs was found.<sup>9</sup> On the other hand, our own preliminary data for size dependent catalytic activity of Pt clusters showed that there is a size dependence as described below. One of the most interesting scientific questions is whether size reduction to that below 1-2 nm can open unprecedented opportunities to fine-tune catalytic properties of these clusters. The idea of employing a unusual chemistry of such ultra-small catalysts can be linked to experimental observations of

extraordinary properties of sub-nm clusters in various heterogeneous reactions; however, the combined effect of light and sub-nm clusters are not well understood.<sup>10-13</sup> Our recent work on Au clusters showed that indeed the strategy of combining sub-nm co-catalysts and light has an enormous promise for increasing the quantum efficiency of photocatalytic H<sub>2</sub> production, where the observed activity enhancements was more than 35 times as compared to that for unmodified catalyst.<sup>14</sup> It is conceivable that similar photocatalytic activity enhancement may be achieved for other noble metals, such as Pt. The rationale of choosing Pt is based on the observation of its superior (to gold) performance in various reactions.<sup>7, 15, 16</sup> Nanometer sized Pt clusters have been found to be efficient co-catalysts for photocatalytic H<sub>2</sub> production,<sup>4</sup> and other reactions, such as electrocatalytic methanol,<sup>17</sup> CO,<sup>18</sup> and 2-propanol<sup>13</sup> oxidation. Our recent work on sub-nm Pt-TiO<sub>2</sub> catalysts for NO<sub>2</sub> oxidation also demonstrated a photocatalytic activity enhancement by about 5 times.<sup>19</sup> All of the above mentioned suggests that combining light and powder supported ultra-small Pt clusters can potentially be a viable strategy for H<sub>2</sub> photocatalytic production, which is the main topic of this paper. In contrast to the above mentioned work on TiO<sub>2</sub>, using the standard catalyst moderately active under visible light, such as CdS, can be employed as a benchmark approach for investigating the effects of sub-nm Pt on H<sub>2</sub> production. It is worth noting that different approaches to improve the catalytic activity of CdS have been reported, e.g. hydrothermal treatment of CdS,<sup>20</sup> controlling morphology of CdS,<sup>21-23</sup> loading of different co-catalysts,<sup>20, 23, 24</sup> and loading CdS on different supporting materials.<sup>23, 25</sup> It is also important to highlight the fact that despite a very extensive literature on using larger Pt particles on standard photocatalysts such as CdS,<sup>26-29</sup> a mechanistic insight on interactions of sub-nm clusters with CdS remains to be explored. It was recently proposed that the cluster size may play a critical role in determining the energy level

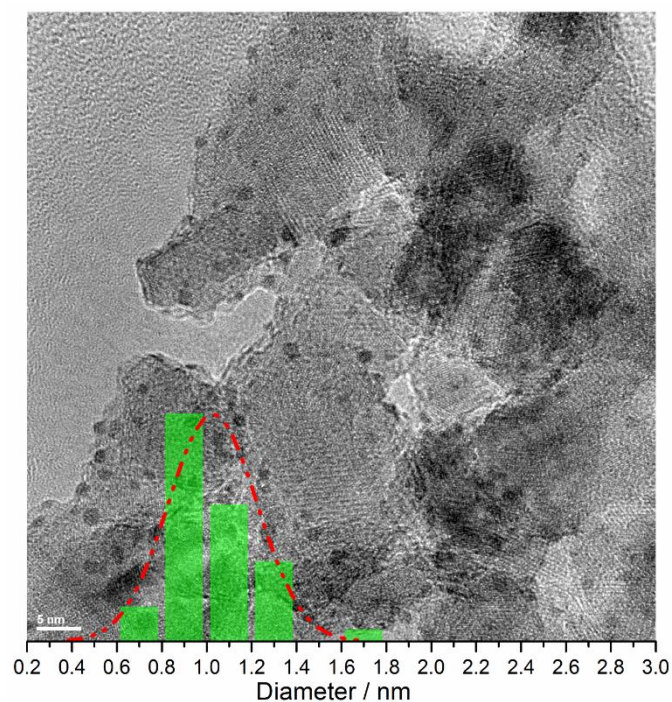


Fig. 1. Transmission electron micrograph of 5 wt% sub-nm Pt loaded on  $\text{Al}_2\text{O}_3$ . Insert is the particle size distribution based on this TEM image showing the average Pt cluster size of  $0.9 \pm 0.1$  nm.

alignment at the cluster/semiconductor interface and in turn the photocatalytic  $\text{H}_2$  production rate.<sup>30</sup> Although experimental data on the electron affinity of sub-nm Pt clusters are not readily available, theoretical studies, such as those based on first-principles density functional theory (DFT) calculation, can help to derive quantitative trends on electron affinity as a function of cluster size and shape. Furthermore, DFT calculations allow investigating the adsorption structures of the supported clusters and probing into the interactions at the cluster/semiconductor interface at the atomic and electronic scale. In this work, we present for the first time combined experimental and DFT studies of CdS supported sub-nm Pt clusters in attempt to understand the structural and electronic interactions at the cluster/semiconductor interface and obtain new insights into role of Pt in photocatalytic  $\text{H}_2$  production

To synthesize Pt nanoparticles we used modified inverse micelle encapsulation approach, which was optimized to produce sub-nm particles. These particles were subsequently deposited on various supports as described in supplementary information. Fig. 1 shows the TEM image and size distribution of supported Pt clusters indicating that the average size of supported sub-nm Pt clusters was about  $0.9 \pm 0.1$  nm. Although Pt particles as big as  $1.7 \pm 0.1$  nm were observed, more than half of all the clusters were in sub-nm range. In order to understand the effect of reducing particle size to nm and sub-nm dimensions on their electronic properties we have conducted DFT calculations of unsupported Pt clusters with diameter in the range of 0.7–1.3 nm (Fig. S1). As expected, the computed binding energy increases towards the bulk value as the size increases as shown in Table S1. The total density of states (DOS) of Pt clusters is shown in Fig. S2. In comparison with bulk Pt, the bandwidth (mostly from  $d$  orbitals) becomes smaller as the cluster size is reduced and the electronic states get more discretized. For all the clusters examined here, the DOS plot demonstrates finite distribution at the vicinity of

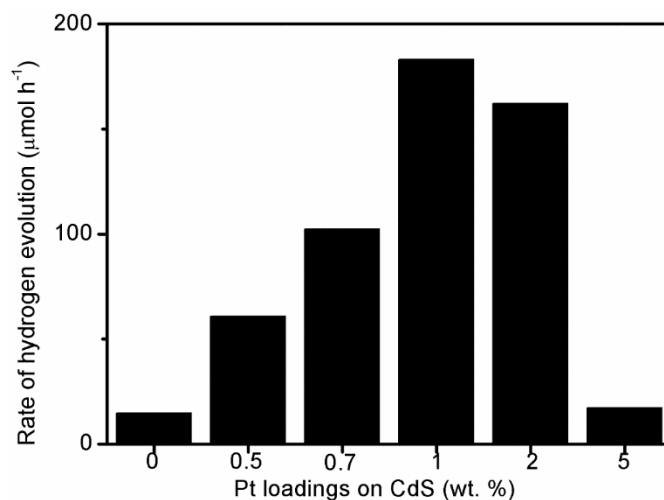


Fig. 2. Rate of  $\text{H}_2$  evolution of CdS with different amount of sub-nm Pt particles loading.

the Fermi level with energy distance between Kohn-Sham HOMO and LUMO energies within 0.1 eV, in sharp contrast to the much larger energy gap found in Au clusters of the same size range. In the context of electron or hole transfer between the Pt cluster and the substrate, the electron removal or addition energy are relevant and the Coulomb charging effects on the cluster have to be considered, which is not included in the Kohn-Sham description of energy levels. Instead, we estimated ionization potential (IP) and electron affinity (EA) of the Pt clusters by taking the total energy difference of the neutral and cationic/anionic Pt clusters. The computed IP and EA values (Table S1) clearly demonstrate a strong size dependence of the excitation energy associated with adding or removing an electron from the Pt cluster. The variation of IP and EA can be roughly fit to the liquid-drop model of metal clusters<sup>31, 32</sup> as  $\text{IP} = \Phi + c_1 e^2/R$  ( $\text{EA} = \Phi + c_2 e^2/R$ ), where  $\Phi$  is the bulk work function,  $c_1$  and  $c_2$  are constants and  $R$  is cluster radius. For clusters in the sub-nm size range, IP and EA can vary by a few hundreds of meV, which may provide a convenient means of tuning the energy level alignment with the band edges of the substrate surface as well as that with the  $\text{H}^+$  reduction potential. In contrast, for large Pt nanoparticles the size dependence is much weaker and only allows a narrow energy window between IP and EA, making it difficult to realize an optimal type-II alignment with the substrate band edges. For example, for a 5 nm Pt nanoparticle, the IP and EA can be extrapolated to be 5.8 eV and 5.2 eV respectively based on our calculations, both falling in the gap of CdS and leading to an unfavorable type I alignment. In addition, for such size range, the EA level is lower than the  $\text{H}^+$  reduction potential, leading to an uphill reduction reaction. Therefore, sub-nm clusters not only satisfy the required energy level alignment with substrate band edges, but also facilitate enhanced photocatalytic activity based on how the EA level is positioned relative to the  $\text{H}^+$  reduction potential.

Following TEM characterization and DFT calculations for unsupported Pt clusters, the Pt modified CdS samples were characterized by XPS and then tested for photocatalytic  $\text{H}_2$  production. XPS spectra are shown in supplementary information (Fig. S3). They indicate that there are two types of Cd species, which might originate from different interactions between CdS and Pt clusters. Further discussion on the interaction between CdS and Pt clusters is presented in supplementary information. Fig. 2 shows the rate of  $\text{H}_2$  evolution

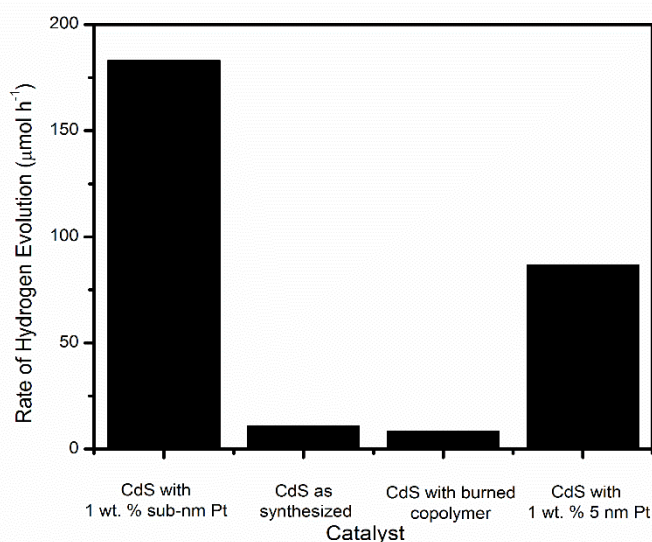


Fig. 3. Rate of  $\text{H}_2$  evolution of CdS with different conditions.

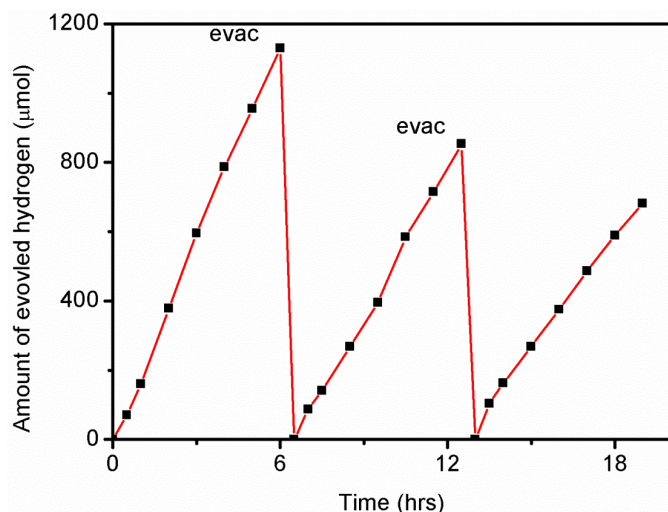


Fig. 4. Stability test for 1 wt% Pt/CdS sample.

on sub-nm Pt/CdS loaded with different amounts of Pt. For comparison purposes, the rate of  $\text{H}_2$  evolution on pure CdS is also presented. These results indicate a substantial improvement of visible light induced  $\text{H}_2$  evolution due to the presence of sub-nm Pt clusters. While the photocatalytic activity of pure CdS was very low ( $11 \mu\text{mol h}^{-1}$ ) as also reported by other groups,<sup>33, 34</sup> the sub-nm Pt modified CdS exhibited a greatly enhanced photocatalytic activity showing almost 17 times improvement in  $\text{H}_2$  evolution rate ( $183 \mu\text{mol h}^{-1}$ ) as compared to that of pure CdS. Such an enhancement was also applicable in quantum efficiency. The optimal activity was observed at 1 wt.% loading. Further increase of Pt loading led to a decrease in photocatalytic activity probably due to the shielding effect of Pt on CdS surface thereby blocking both light and reactant access to semiconductor surface. In order to confirm that this catalytic performance improvement is not coming from surface sensitization with polymer residues and to compare activity of sub-nm Pt with larger Pt NPs, we have conducted additional control experiments. Fig. 3 shows the rate of  $\text{H}_2$  evolution on CdS samples prepared in several different ways. The lowest activity was observed for CdS samples with burned copolymer where no Pt was deposited in order to evaluate the effect of polymer on catalytic activity. This low activity can

be explained perhaps by simultaneous presence of polymer residues blocking catalytic surface and formation of CdO from CdS. Importantly,  $\text{H}_2$  evolution rates on sub-nm Pt sample was still 2 times higher than that for the samples containing larger ( $\sim$  aver. 5 nm) Pt particles. Fig. 4 shows the  $\text{H}_2$  evolution rate of the 1 wt. % Pt loaded CdS as a function of time. Three cycles of photocatalytic activity tests were conducted to determine long-term stability and activity of this sample. The sample showed nearly linear rate of  $\text{H}_2$  evolution for all three cycles with only small deactivation of the sample observed at the end of the 18 hours run (Fig. 4). This deactivation may be attributed to the aggregation of sub-nm Pt clusters to larger clusters and the photocorrosion of CdS.<sup>35</sup> Given our previous work with CdS,<sup>14</sup> and the presence of sacrificial reagents, the surface photocorrosion of CdS is most likely a minor factor as compared to Pt segregation. TEM images of samples before and after activity testing are shown in supplementary information (Fig. S4 and Fig. S5). By comparing Fig. S4 and Fig. S5, a noticeable segregation of Pt was observed, supporting the above mentioned conclusion.

The origins for catalytic activity improvements for Pt clusters supported on CdS surfaces have been discussed in the literature. For larger than 1 nm Pt clusters, several effects can be considered. The first one is the cluster size, where keeping the Pt loading constant while decreasing particle size results in increase in the cluster density. Considering this effect alone without taking into account the nature of cluster interactions with the surface and change in their electronic properties can be misleading. For example, Jun and coworker's found<sup>9</sup> that the enhanced photocatalytic activity cannot be simply correlated to just an increase in cluster number density originating from their smaller size at a given Pt loading. Another effect is related to energy level alignments between Pt and CdS. Wu *et al.* invoked the consideration of the initial formation of electron-hole pairs and subsequent long-lived separation of charge carriers to explain the activity enhancement, and suggested that the observed long life time of the charge separated state and the reduced carrier recombination rate were caused by the trapping of holes in CdS.<sup>29, 36</sup> Schweinberger *et al.* proposed a thermodynamic model for the energy level alignment at the cluster/CdS interface, and suggested that there exists an optimal energy position of the Pt cluster LUMO in between the conduction band minimum (CBM) of CdS, and hydrogen reduction potential so that the photoexcited electrons can be efficiently transferred *downhill* from the CdS CBM to the cluster LUMO and then to the proton.<sup>30</sup> However, there is no direct experimental or theoretical evidence to support such a simple thermodynamic model. First, experimental measurements of the electron affinity of sub-nm Pt clusters, either bare or supported on CdS, are not readily available from the literature. More importantly, such a simple picture of energy level alignment neglects the fact that interactions between the Pt cluster and the underlying substrate may have a significant influence on their geometry and electronic structure, which can modify energy level alignment at the interface and affect the hydrogen production activity of the system. Therefore, in order to examine the nature of such interactions at the cluster/substrate interface, we carried out DFT calculations for adsorption of a  $\text{Pt}_{38}$  cluster on the nonpolar CdS ( $10\bar{1}0$ ) surface. Multiple Pt-S and Pt-Cd bonds are formed at the interface, and an adsorption energy of  $-10.7 \text{ eV}$  was computed from the total energy difference of the unsupported Pt cluster, the clean CdS ( $10\bar{1}0$ ) surface and the adsorption system, all individually relaxed. The optimized

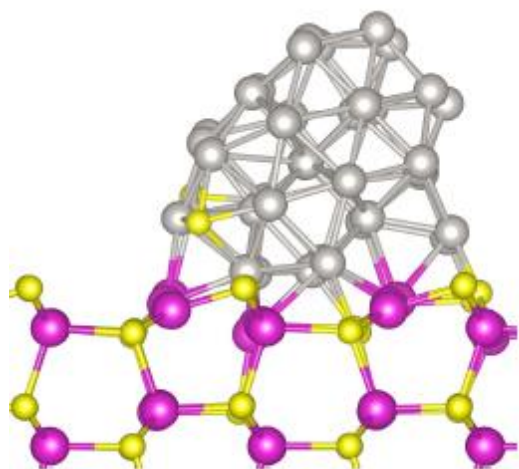


Fig. 5. DFT-optimized geometry of Pt<sub>38</sub> on CdS (10 $\bar{1}$ 0) surface. For clarity, only the top four atomic layers of the substrate are shown. Silver, magenta and yellow spheres represent Pt, Cd and S atoms respectively.

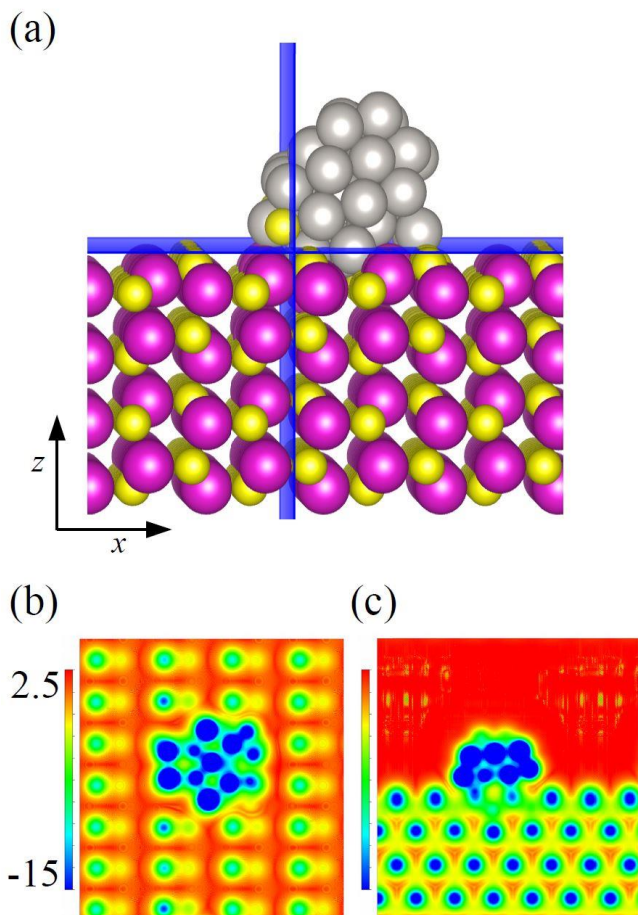


Fig. 6. Contours of electrostatic surface potential of Pt<sub>38</sub>/CdS on cutting planes that are normal to: (b) z-axis and (c) x-axis, as highlighted by blue in the structural model in (a). z- and x-axes are along the [10 $\bar{1}$ 0] and [0001] directions, respectively. Potential energies are in eV.

structure is shown in Fig. 5, which reveals large structural distortion of the Pt<sub>38</sub> cluster from its initial O<sub>h</sub> symmetry. The crystallinity of the cluster was substantially reduced, with deformation energy as high as 3.0 eV. In addition, structural distortion of the substrate accompanied with atomic diffusion of surface sulfur atoms into the Pt<sub>38</sub> cluster are observed, resulting in large deformation energy of the substrate (10.5 eV). The geometry deformation (of both the cluster and the substrate) and interfacial bonding are expected to substantially influence the electronic structure of the interface. For example, we found that the electron affinity of Pt<sub>38</sub> in the deformed geometry changes by as much as 0.6 eV compared to that in the gas phase. In addition, the calculation of surface dipole moment indicated an overall electron flow from CdS surface to Pt cluster, which may locally modify the surface potential and influence the electronic structure. Contour plots of calculated effective surface potential of Pt<sub>38</sub>/CdS (10 $\bar{1}$ 0) are shown in Fig. 6, which clearly demonstrates the variation of surface potential near the region where the cluster comes in contact with the substrate. A more systematic study is under way to understand the qualitative and quantitative trend of such potential shifts. Whereas an accurate picture of the energy level alignment at the interface cannot be achieved within the Kohn-Sham picture of DFT and is not in the scope of this paper, our DFT results highlights the importance of going beyond the simple picture based on clean (or bulk) CdS substrate and unsupported Pt clusters and explicitly treating the interface with realistic structural model.

## Conclusions

In conclusion, we reported a first ever observation of exceptional photocatalytic hydrogen production activity of sub-nm Pt clusters modified CdS NPs system by combining TEM and photocatalytic measurements. The experimental results showed almost 17 times improvement in H<sub>2</sub> evolution rate as compared to that for unmodified surface. This performance was also significantly better performance as compared to that for 5 nm Pt particles. To provide mechanistic insight on such enhancement, we carried out DFT calculation of both unsupported Pt clusters and absorption of Pt clusters on CdS surface. Our results revealed strong structural and electronic interaction between clusters and substrate, which may substantially influence the electronic structures of both sub-nm Pt cluster and CdS surface, as well as the local surface potential. We believe that this is the first ever work offering such mechanistic insight into behavior of supported sub-nm Pt clusters. The resulting electronic structure of the cluster/semiconductor interface may be the key component of significant enhancement of photocatalytic hydrogen production activity of this system. Given the difficulty of directly measuring such properties from experiments, our work offered new and important views to understanding the complicated stories behind this exceptional photocatalytic activity.

## Acknowledgement

Alexander Orlov would like to acknowledge financial support from the NSF DMR award #1231586. Work performed by Shangmin Xiong, Yan Li and Dong Su was supported by the U.S. Department of Energy, Office of Basic Energy Sciences, under Contract No. DE-AC02-98CH10086. TEM measurements and DFT calculations were carried out at the Center for Functional Nanomaterials at Brookhaven

National Laboratory, which is supported by the U.S. Department of Energy, Office of Basic Energy Sciences, under Contract No. DE-AC02-98CH10886. This research also used resources of the National Energy Research Scientific Computing Center, a DOE Office of Science User Facility supported by the Office of Science of the U.S. Department of Energy under Contract No. DE-AC02-05CH11231. We would also like to thank Dr. Mike White for his help in XPS experiment.

## Notes and references

<sup>a</sup> Department of Material Science and Engineering, Stony Brook University, Stony Brook, New York 11794, USA.

Email: alexander.orlov@stonybrook.edu

<sup>b</sup> Computational Science Center, Brookhaven National Laboratory, Upton, New York 11973, USA

<sup>c</sup> Center for Functional Nanomaterials, Brookhaven National Laboratory, Upton, New York 11973, USA.

Electronic Supplementary Information (ESI) available: Experimental methods, DFT calculation details and data of unsupported Pt clusters. See DOI: 10.1039/c000000x/

1. K. Maeda and K. Domen, *Journal of Physical Chemistry C*, 2007, 111, 7851-7861.
2. A. Kudo and Y. Miseki, *Chemical Society Reviews*, 2009, 38, 253-278.
3. K. Maeda and K. Domen, *Journal of Physical Chemistry Letters*, 2010, 1, 2655-2661.
4. S. Sato and J. M. White, *Chem. Phys. Lett.*, 1980, 83.
5. J. M. Lehn, J. P. Sauvage and R. Ziessel, *Nouveau Journal De Chimie-New Journal of Chemistry*, 1980, 4, 623-627.
6. K. Yamaguti and S. Sato, *Journal of the Chemical Society-Faraday Transactions I*, 1985, 81, 1237-1246.
7. G. R. Bamwenda, S. Tsubota, T. Nakamura and M. Haruta, *Journal of Photochemistry and Photobiology a-Chemistry*, 1995, 89, 177-189.
8. A. Iwase, H. Kato and A. Kudo, *Catalysis Letters*, 2006, 108, 7-10.
9. J. Xing, Y. H. Li, H. B. Jiang, Y. Wang and H. G. Yang, *International Journal of Hydrogen Energy*, 2014, 39, 1237-1242.
10. J. D. Aiken and R. G. Finke, *Journal of Molecular Catalysis a-Chemical*, 1999, 145, 1-44.
11. M. Couillard, R. E. Palmer and P. D. Nellist, Dundee, Scotland, 2001.
12. J. H. Kang, L. D. Menard, R. G. Nuzzo and A. I. Frenkel, *Journal of the American Chemical Society*, 2006, 128, 12068-12069.
13. S. Mostafa, F. Behafarid, J. R. Croy, L. K. Ono, L. Li, J. C. Yang, A. I. Frenkel and B. R. Cuenya, *Journal of the American Chemical Society*, 2010, 132, 15714-15719.
14. P. C. Shen, S. Zhao, D. Su, Y. Li and A. Orlov, *Applied Catalysis B-Environmental*, 2012, 126, 153-160.
15. Y. Mizukoshi, Y. Makise, T. Shuto, J. Hu, A. Tominaga, S. Shironita and S. Tanabe, *Ultrasonics sonochemistry*, 2007, 14, 387-392.
16. E. Gyenge, *Electrochimica Acta*, 2004, 49, 965-978.
17. E. Yoo, T. Okata, T. Akita, M. Kohyama, J. Nakamura and I. Honma, *Nano Letters*, 2009, 9, 2255-2259.
18. E. Yoo, T. Okada, T. Akita, M. Kohyama, I. Honma and J. Nakamura, *Journal of Power Sources*, 2011, 196, 110-115.
19. S. Zhao, G. Ramakrishnan, P. C. Shen, D. Su and A. Orlov, *Chemical Engineering Journal*, 2013, 217, 266-272.
20. J. H. Yang, H. J. Yan, X. L. Wang, F. Y. Wen, Z. J. Wang, D. Y. Fan, J. Y. Shi and C. Li, *Journal of Catalysis*, 2012, 290, 151-157.
21. Q. J. Xiang, B. Cheng and J. G. Yu, *Applied Catalysis B-Environmental*, 2013, 138, 299-303.
22. J. Jin, J. G. Yu, G. Liu and P. K. Wong, *J Mater Chem A*, 2013, 1, 10927-10934.
23. A. Sathish and R. P. Viswanath, *Catal Today*, 2007, 129, 421-427.
24. S. Chen, X. P. Chen, Q. Z. Jiang, J. Yuan, C. F. Lin and W. F. Shangquan, *Appl Surf Sci*, 2014, 316, 590-594.
25. X. X. Zhou, H. R. Chen, Y. Y. Sun, K. Zhang, X. Q. Fan, Y. Zhu, Y. Chen, G. J. Tao and J. L. Shi, *Applied Catalysis B-Environmental*, 2014, 152, 271-279.
26. L. A. Silva, S. Y. Ryu, J. Choi, W. Choi and M. R. Hoffmann, *Journal of Physical Chemistry C*, 2008, 112, 12069-12073.
27. J. S. Jang, S. H. Choi, H. G. Kim and J. S. Lee, *Journal of Physical Chemistry C*, 2008, 112, 17200-17205.
28. H. Yan, J. Yang, G. Ma, G. Wu, X. Zong, Z. Lei, J. Shi and C. Li, *Journal of Catalysis*, 2009, 266, 165-168.
29. K. Wu, H. Zhu, Z. Liu, W. Rodriguez-Cordoba and T. Lian, *Journal of the American Chemical Society*, 2012, 134, 10337-10340.
30. F. F. Schweinberger, M. J. Berr, M. Doeblinger, C. Wolff, K. E. Sanwald, A. S. Crampton, C. J. Ridge, F. Jaeckel, J. Feldmann, M. Tschurl and U. Heiz, *Journal of the American Chemical Society*, 2013, 135, 13262-13265.
31. M. Seidl, M. E. Spina and M. Brack, *Z Phys D Atom Mol Cl*, 1991, 19, 101-103.
32. E. I. S. Xiong, Y. Li, *submitted*, 2014.
33. X. Zong, H. Yan, G. Wu, G. Ma, F. Wen, L. Wang and C. Li, *Journal of the American Chemical Society*, 2008, 130, 7176-+.
34. H. Park, W. Choi and M. R. Hoffmann, *Journal of Materials Chemistry*, 2008, 18, 2379-2385.
35. N. Bao, L. Shen, T. Takata and K. Domen, *Chemistry of Materials*, 2008, 20, 110-117.
36. K. F. Wu, Z. Y. Chen, H. J. Lv, H. M. Zhu, C. L. Hill and T. Q. Lian, *Journal of the American Chemical Society*, 2014, 136, 7708-7716.